HIGH POWER FACTOR ELECTRONIC LIGHTING SYSTEM EMPLOYING THE SEPIC AND HALF-BRIDGE INVERTER FOR AC POWER LEDS

LUIZ H. OKIDA AND CLAUDINOR B. NASCIMENTO

Department of Electrical Engineering, Federal University of Technology of Parana, Campus Ponta Grossa
Avenida Monteiro Lobato, Km 04, S/N, Jardim Pitangui, Ponta Grossa, PR – CEP 84016-210
E-mails: luizokida@gmail.com; claudinor@utfpr.edu.br

Abstract— The use of LEDs that operate in alternating current (ac) can be considered with a good solution for lighting system applications. With high direct breakdown voltage and low driving current, through a resistor element, the AC power LEDs can be directly connected to the power supply. However, the direct connection in the power supply produces a high harmonic distortion in input current and the IEC 61.000-3-2 is not attended. This paper presents the study of an electronic lighting system with power factor correction (PFC) to drive AC power LEDs employing the SEPIC converter associated to the Half-Bridge voltage inverter. SEPIC converter carries out the power factor correction and DC bus voltage regulation. Half-Bridge inverter operating with asymmetrical PWM gate pulses, i.e., using I–LFSQW (Low Frequency Square Wave Current) technique, carries out the reversal of voltage and current in the load. Simulation results for two conduction modes (DCM-Discontinuous Conduction Mode and BCM-Boundary Conduction Mode) and experimental results for DCM are presented.

Keywords— AC Power LEDs, SEPIC converter, Half-Bridge inverter, Power Factor Correction.

1 Introduction

LED lighting systems are increasingly being used to replace conventional lamps such as fluorescent and HPS. Besides LEDs have been mainly used on traffic light, indoor lighting, lighting of architectural environments and full colors display, their applications like lamps is rising significantly in recent years [1 -2]. More recently, also for use in lighting system, appear the light emitting diodes for alternating current, i.e., the AC LEDs [3-12]. Compared to the DC LEDs, the AC LEDs have as main advantages the higher power production with low levels driving currents. Thus, it is possible to perform parallel associations of these LEDs to increase the luminous flux of the system. With direct high breakdown voltage operation, they can be connected directly to the power supply through of a resistor or a capacitor. On the other hand, their lifetime goes up to 50,000 hours [13], against 100,000 hours of DC LED. When a resistor is used to limit AC LEDs current, it has two problems, e.g., the losses in resistor and high harmonic distortion in input current due to its high breakdown voltage [11-13]. Figure 1 (a) showsthe AC LED connected on the power supply using only a resistor. High harmonic distortion in the input current can be observed from the Figure 1 (b).

One of the possible ways to reduce the harmonic distortion of the input current and improve the overall efficiency of the system it is through of use of an AC-AC switched power converter. However, the employed AC-AC circuit should ensure that some operational features such as the low frequency alternating current and constant output power are preserved over all livespan of the AC LEDs.

Single-stage topologies based on the half-bridge converter present a reduced number of components and high efficiency as main advantages [14].

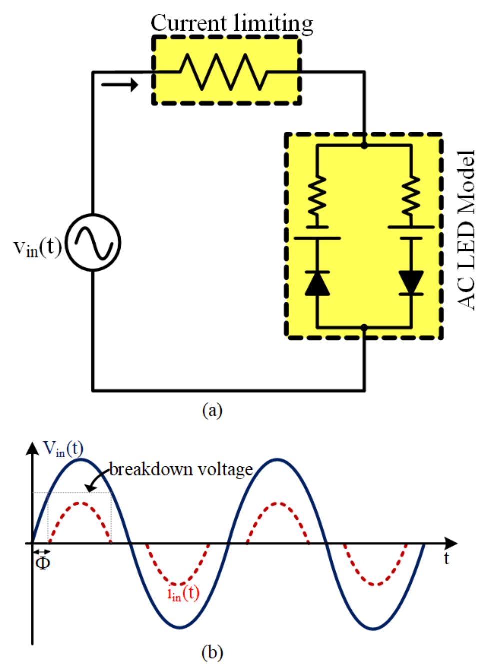

Figure 1. AC LEDs circuits with limiter resistor and their input voltage and current waveform.

However, the output voltage regulation is not easily obtained and the control output power is usually performed by switching frequency range employing symmetrical gate pulse. When the asymmetrical PWM is employed, an additional circuitry for detecting the input voltage semi cycle is necessary in order for generating a switching pattern [17]. Two-stage topologies have the output voltage and power regulations facilited. However, the system overall efficiency can be affeted.

This paper presents the sudy of an electronic lighting system for AC LEDs device. The proposed topology employs a SEPIC converter associated to the output voltage half-bridge inverter. SEPIC configuration perfoms the PFC (power factor corrrection) and DC-link voltage regulation while the half-bridge inverter provides the low frequency alternating current for the AC LEDs. In order to obtained a low frequency square waveform current in the LEDs, an asymmetrical PWM strategy as gate pulses for the inverter switches is employed [14-16]. In addition, aiming to observe the system efficiency the SEPIC is simulated at Boundary and Discontinuos Conduction Modes. Experimental results for DCM.

2 Proposed Topology

Proposed two-stage converter is shown in Figure 2. The feeding of the AC LED is made by a half-bridge voltage inverter controlled by I-LFSQW technique [14]. Figure 3 illustrates the instantaneous currents in the L_o inductor in BCM and DCM operations.

From the Figure 1 it can be observed that the AC LED current is null for a long interval of time. Thus, to maintain the output average power the current peak value is higher. In this case, during the time which the LEDs are reenergized, the luminous flux and components lifetime is reduced. To resolve this problem, it is proposed to feed the LEDs with square waveform using the I-LFSQW technique.

Table 1 shows the Total Harmonic Distortion (THD) of the input current and Power Factor (PF) performance comparison between the circuit presented in the Figure 1 and the proposed lighting system at DCM and BCM conditions for 48 W output power (10 parallel AC LEDS). It can observe that the values of the circuit of the Figure 1 do not meet the IEC 61.000-3-2 Class C standard.

Figure 4 illustrates, in simplified form the PWM strategy used in S_1 and the Figure 5 shows the PWM strategy for the switches S_2 and S_3 of the voltage inverter.

Table 1. THD and PF performance comparison between the circuit presented in the Figure 1 and the proposed lighting system at DCM and BCM conditions.

Topologies	THDi (%)	PF
Circuit of the Figure 1	30.5	0.899
Proposed converter at DCM	10.3	0.992
Proposed converter at BCM	8.6	0.996

3 Steady-State Operation

Principle of operation in DCM at steady state of the presented topology is characterized by six operating stages. The analyses performed in this paper take into consideration the following assumptions:

- The operations stages and theoretical waveforms are presented for duty cycle (D) on the switches S_1, S_2 and S_3 at switching frequency and peak value of the grid voltage;
- The voltage on capacitor C_1, disregarding its high-frequency ripple, is equal to input voltage $v_{in}(t)$;
- The voltages on capacitors C_2 and C_3 are equal to half the dc-link voltage and equal to V_{DC}. It is considered that $C_2 = C_3 = C_{DC}$;
- The performed analyses for switching frequency of S2 and S3 is twice the switching frequency of S1.

A Description of the Operation Stages

The operation stages description can be carried out considering the following conditions:

1 - S_1 turned-on and D_1 turned-off: In this operating condition, the SEPIC converter does not provide current to the bus capacitors neither to the AC LEDs. Also, in this operation condition, C_2 provides

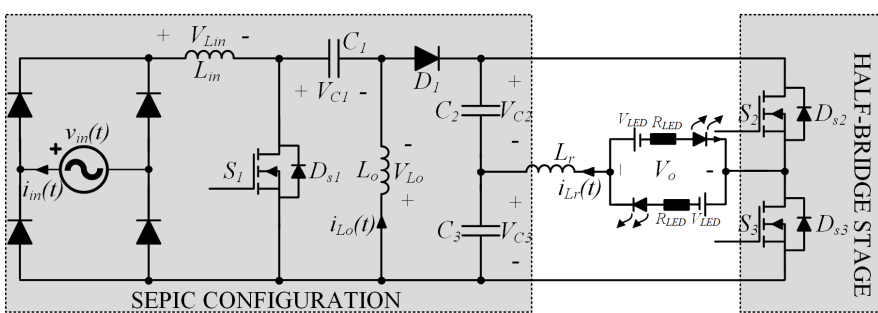

Figure 2. Proposed two-stage converter.

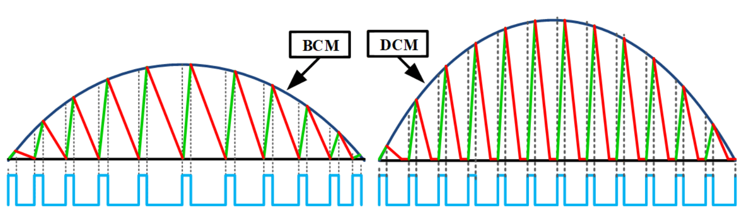

Figure 3. L_o inductor currents in BCM and DCM operations.

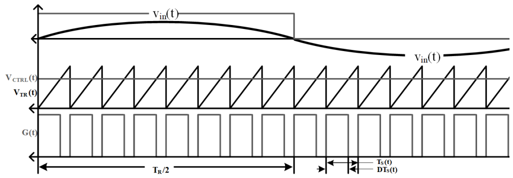

(a) PWM strategy

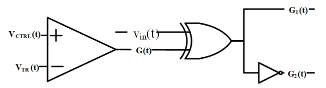

(b) Logic circuit for PWM strategy implementation.

Figure 4. PWM strategy used in the two-stage converter.

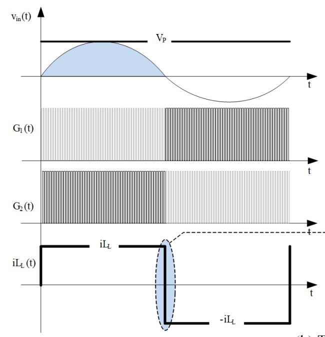

(a) Ideal waveforms at grid frequency

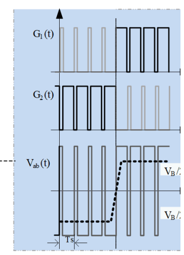

(b) Transition detail of output hal voltage at swiching grequen

Figure. 5. Switches S_2 and S_3 gate pulses.

energy for the AC LEDs when S_2 is turned-on and C_3 receives energy from L_r while D_{s3} conducts. The Figure 6 (a) and Figure 6 (b) show these operation conditions.

2 - S_1 turned-off and D_1 turned-on: In this operating condition, all energy stored by L_{in} and L_o in the two previous stages are provided for the bus capacitors C_2 and C_3 as well to the AC LEDs as illustrated by Figure 6 (c) and Figure 6 (d).

3 - S_1 turned-off and D_1 turned-off: Finally, in this operating condition, there is no energy storage by L_{in} and L_o and the output stage operates according to description of the two first operating stages. Figure 6 (e) and Figure 6 (f) presents this operating condition.

It can be observed the previous six operation stages occur for a positive output current. With reversal of the PWM pulses applied to the switches S_2 and S_3, the output current becomes negative and only the switch S_3 and the diode D_{s2} start driving. Regarding to the operation of the SEPIC in BCM, only the operation conditions 1 and 2 should be considered.

Fig. 7 presents the key theoretical waveforms at steady state for DCM and BCM operation.

B Mathematical Analysis

One of the advantages of two-stage topologies is that their mathematical model can be independently obtained. Therefore, in this work, when analyzing the operation stages presented in Figure 6, with the SEPIC working at DCM the following equations are found:

$$I_{inM,DCM} = \frac{V_p D_{s1}\left[L_{in} D_{s1} V_{DC} + L_o\left(2V_{DC} - D_{s1} V_{in}\right)\right]}{2 L_{in} L_o V_{DC} f_{s1}} \quad (1)$$

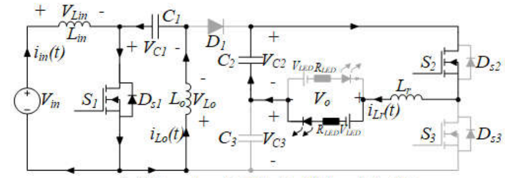

(a) Stage 1 – S_1 ON, D_1 OFF and S_2 ON

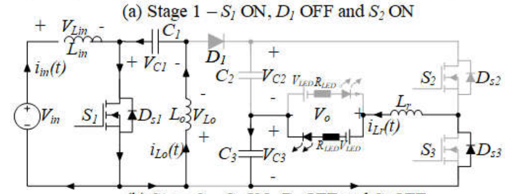

(b) Stage 2 – S_1 ON, D_1 OFF and S_2 OFF

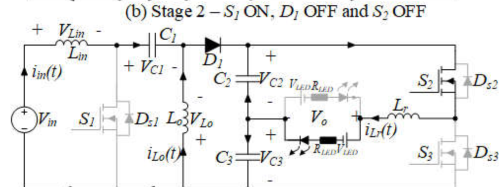

(c) Stage 3 – S_1 OFF, D_1 ON and S_2 ON

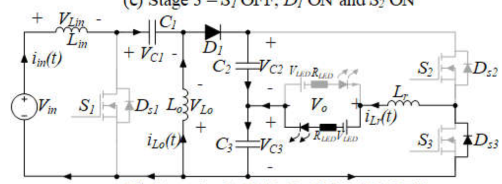

(d) Stage 4 – S_1 OFF, D_1 ON and S_2 OFF

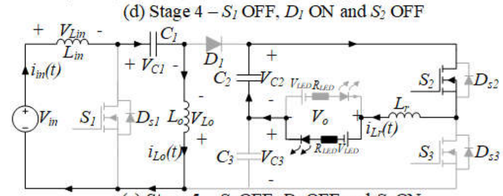

(e) Stage 5 – S_1 OFF, D_1 OFF and S_2 ON

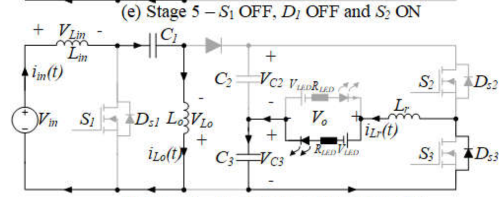

(f) Stage 6 – S_1 OFF, D_1 OFF and S_2 OFF

Figure 6. Operation Stages at DCM.

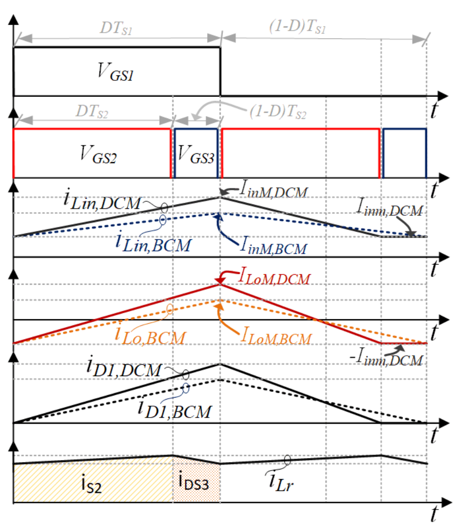

Figure 7. Key theoretical waveforms at steady state.

$$I_{inm,DCM} = \frac{V_p D_{s1}{}^2 \left[L_{in} V_{DC} + L_o V_p \right]}{2 L_{in} L_o V_{DC} f_{s1}} \quad (2)$$

$$I_{LoM,DCM} = \frac{V_p D_{s1} \left[L_{in} V_{DC} \left(2 - D_{s1}\right) + L_o D_{s1} V_{in} \right]}{2 L_{in} L_o V_{DC} f_{s1}} \quad (3)$$

$$I_{in,avg} = \frac{V_p D_{s1}{}^2 \left(L_{in} + L_o \right)}{2 L_{in} L_o f_{s1}} \quad (4)$$

$$P_{in,avg} = \frac{V_p^2 D_{s1}{}^2 \left(L_{in} + L_o \right)}{2 L_{in} L_o f_{s1}} \quad (5)$$

From equation (5), it is possible to note the input average power of the SEPIC converter does not depend on the load. Thus, in output load variation conditions, in order to provide constant input average power, the dc-link voltage will be naturally changed. In lighting system applications employing LEDs, it can be one advantage because the LEDs produces a lower luminous flux as it grows older.

In BCM mode, the following equations are given:

$$I_{inM,BCM} = \frac{V_p D_{s1} \left[L_{in} D_{s1} + L_o \left(1 + D_{s1}\right) \right]}{2 L_{in} L_o f_{s1}} \quad (6)$$

$$I_{inm,BCM} = \frac{V_p D_{s1} \left[L_{in} D_{s1} + L_o \left(1 - D_{s1}\right) \right]}{2 L_{in} L_o f_{s1}} \quad (7)$$

$$I_{LoM,BCM} = \frac{V_p D_{s1} \left[L_{in} \left(2 - D_{s1}\right) - L_o \left(1 - D_{s1}\right) \right]}{2 L_{in} L_o f_{s1}} \quad (8)$$

$$I_{in,avg} = \frac{V_p D_{s1}{}^2 \left(L_{in} + L_o \right)}{2 L_{in} L_o f_{s1}} \quad (9)$$

$$P_{in,avg} = \frac{V_p^2 D_{s1}{}^2 \left(L_{in} + L_o \right)}{2 L_{in} L_o f_{s1}} \quad (10)$$

4 Design Procedure

The elements L_{in}, C_1 and L_o of the SEPIC converter can be designed as a common SEPIC PFC rectifier [18]-[19].

The first step of the design of DCM SEPIC is choose a properly load given by equation (11).

$$R = \frac{V_o^2}{P_o} \quad (11)$$

The L_{in} inductance is obtained by the equation (12).

$$L_{in} = \frac{D_{s1} \cdot V_{in\_peak}}{\Delta i_{in} \cdot I_{in,avg} \cdot f_{s1}} \quad (12)$$

The L_o inductance is given by equation (13).

$$L_o = \frac{L_{in} \cdot R \cdot V_p^2 \cdot D_{s1}^2}{4 \cdot L_{in} \cdot V_{DC}^2 \cdot f_{s1} - R \cdot V_p^2 \cdot D_{s1}^2} \quad (13)$$

The C_1 capacitance is obtained by equation (14).

$$C_1 = \frac{D_{s1}^2 V_p [D_{s1}(V_p L_o - V_{DC} L_{in}) + 2 V_{DC} L_{in}]^2}{2 V_{DC}^2 L_{in}^2 L_o \Delta V_{DC} f_{s1}^2} \quad (14)$$

For BCM conditions, the first step is to define the $D_{s1\_critical}$ at the voltage peak given by equation (15).

$$D_{s1\_critical} = \frac{V_o}{(V_{in\_peak} + V_o)} \quad (15)$$

The inductances and capacitance at BCM can be calculated using the same equations obtained in DCM. However, the switching frequency f_s is the minimum frequency that occurs at voltage peak of the input voltage.

Regarding to half-bridge design, their parameters can be defined employing the same methodology of the Buck converter, as shown in equation (16).

$$L_r = \frac{V_{DC} D_{s2}}{2 f_{S2} \Delta i_{Lr}} \quad (16)$$

The integration of the SEPIC converter and half-bridge inverter is made by dc-link capacitors C_2 and C_3. However, the individual capacitance value must be twice the obtained dc-link capacitance value for SEPIC converter, in order to keep the same voltage ripple on the load. The SEPIC capacitor is obtained by the hold-up time criteria given by equation (17).

$$C_{DC} = \frac{2 P_o th}{V_{DC\_Link}^2 - (0.9 V_{DC\_Link})^2} \quad (17)$$

5 Results

In order to verify the circuit operation in both DCM and BCM conditions of the proposed electronic lighting, a 48 W output AC LED driver has been designed and simulated. Table 2 presents the design specifications and the Table 3 the list of main circuit parameters and selected components.

Figure 8 shows the input voltage and current for both boundary and discontinuous conduction modes. It can be observed the high-power-factor and low THDi for two conduction modes. The simulated THDi

Table 2. Design specifications.

Parameter	Value
Input voltage v_{in}	127 V
Output voltage V_{out}	127 V
DC-link voltage V_{DC}	254 V
Output Power P_{out}	48 W
SEPIC switching frequency f_{s1}	50 kHz
Duty cycle D_{s1}	50%
Half-Bridge Switching frequency f_{s2}	100 kHz
Duty cycle D_{s2} for S_2 at positive semi-cycle	30%
Δi_{in}	20% of $I_{in,avg}$
ΔV_{DC}	10% of Vp

Table 3. List of main circuit parameters and selected components.

Parameter	Value
D_{R1} - D_{R4}	1N4007
D_1	MUR160
S_1, S_2 and S_3	SPP24N60C3V
L_{in}	12.5 mH
L_o	800 µH
C_1	470 nF/ 450 V
C_2=C_3	2 x 82 µF / 250 V
L_r	3.5 mH
LEDs	(10 // LEDs) AN3200 – 120 V / 40 mA

and FP for both operation modes are 10.3% and 0.99 for DCM and 8.6% and 0.99 respectively. As expected, the input current for DCM (Figure 8 (a)) is higher than the input current in BCM (Figure 8 (b)).

Figure 9 presents the output voltage and current for both modes. A low frequency square waveform is verified for two modes too. The positive-to-negative transition detail is shown in the Figure 10 (a) and 10 (b). From Figure 10 it can be noted that the switching frequency of BCM is higher than the DCM.

The C_1 voltage and L_o current at grid frequency are shown in the Figure 11. The L_o current detail at switching frequency is illustrates in the Figure 12. From figures 11 and 12 it can be observed that the current peak value in BCM is lower than in DCM, thus a better efficiency should be obtained for BCM operation.

The dc-link voltage and D_1 current are presented in the Figure 13, firstly at nominal load (Figures (b) and (a)) and after for 50 % of the LEDs resistance (Figures (c) and (d)) for DCM and BCM conditions. From these Figures it can note that the dc-link voltage naturally changes for load variations, in order to insure the constant input and output power. This circuit operational feature it is very appropriated in some applications such as lighting.

Finally, the Figure 14 presents some experimental results with the system operating at DCM according

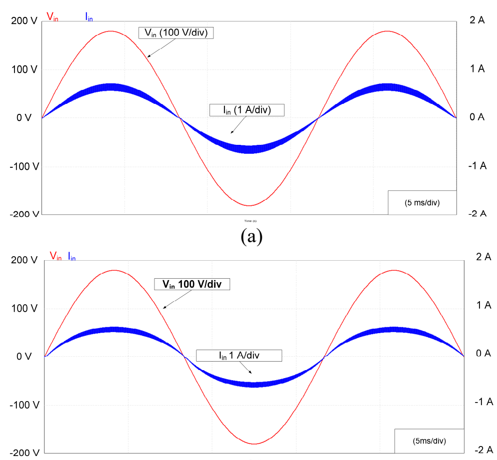

(a)

(b)

Figure 8. Input voltage and current: (a) DCM; (b) BCM.

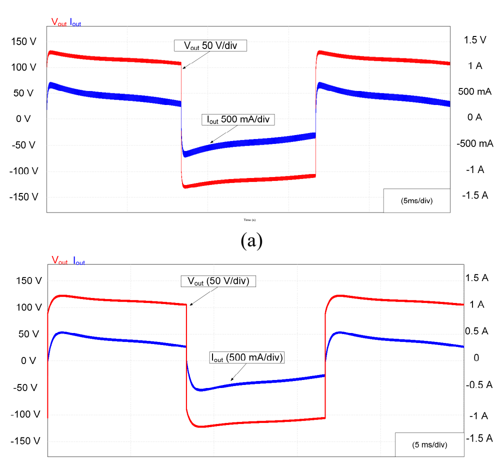

(a)

(b)

Figure 9. Output voltage and current: (a) DCM; (b) BCM.

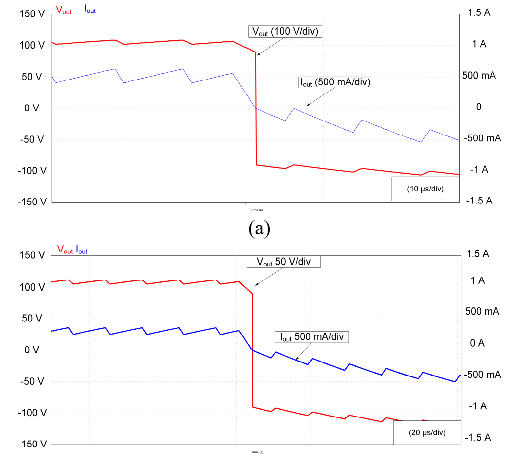

(a)

(b)

Figure 10. Positive-to-negative output voltage and current transition detail in the input voltage peak value: (a) DCM; (b) BCM.

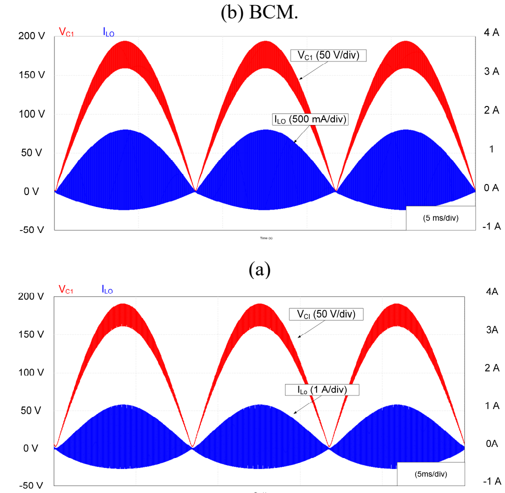

(a)

(b)

Figure 11. C_1 voltage and L_o current at grid frequency: (a) DCM; (b) BCM.

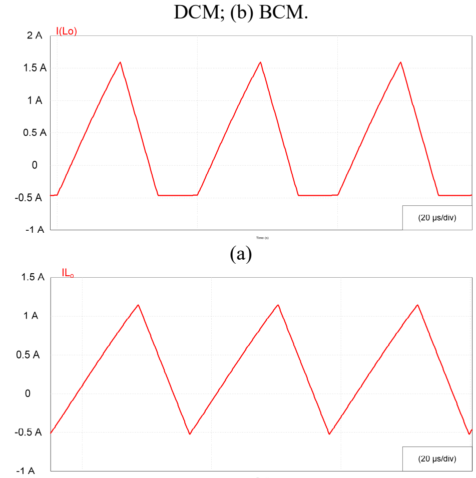

(a)

(b)

Figure 12. L_o current detail at switching frequency: (a) DCM; (b) BCM.

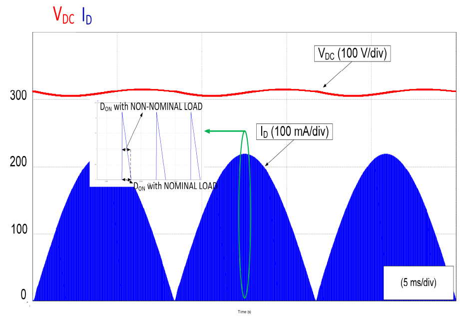

(a)

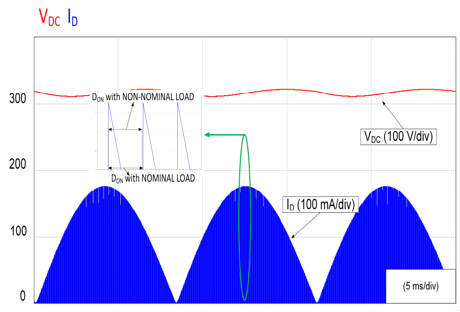

(b)

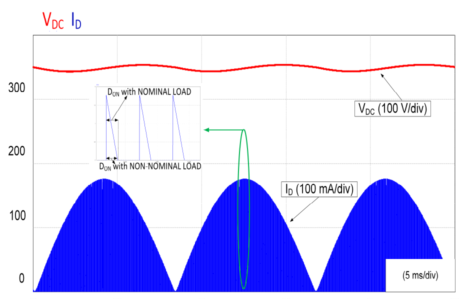

(c)

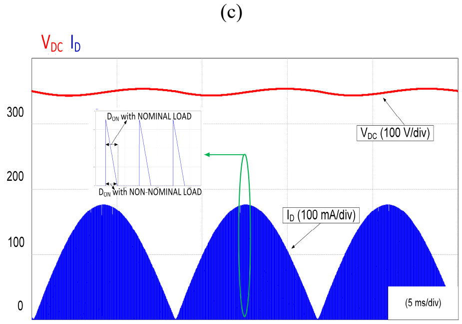

(d)

Figure 13. DC-link voltage and D_1 current: (a) - DCM and (b) BCM at nominal outoput load; (c) - DCM and (d) - BCM at 70 % of the output load.

to the data presented in the Table 2. It is possible to observe that both the input and the output characteristics are similar to the previous presented simulation results. The measured THDi and PF of the input power source are 11% and 0.99, respectively. The obtained overall system efficiency was around of 90 %, which corresponding to 95% for each individual stage. Therefore, the proposed lighting system can be considered as an appropriate circuit to driver and control AC power LEDs.

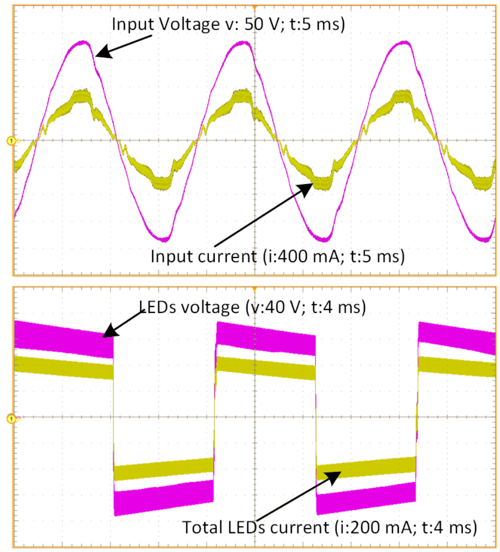

Figure 14. – Input voltage and current of the power supply and voltage and total current on the AC LEDs in DCM.

6 Conclusion

A two-stage converter with power factor correction to drive and control AC power LEDs is presented in this paper. The BCM mode is used in SEPIC converter to increase system efficiency. I-LFSQW technique is used as gate pulses for switches S_2 and S_3 of the half-bridge voltage. AC LEDs have been presenting as a good choice in applications for public and residential lighting systems. The preliminary simulation results show at BCM it has a lower peak current, thus the system overall efficiency should be improved. Future studies may show that one can apply universal input supplier, and it dimmed to control the luminous flux emitted by the LEDs. All system analysis will be presented in the final version in this paper.

References

[1] Carvalho, H. M. B. “Diodos Emissores de Luz de Alto Brilho e Alta Potência”. Directlight – Artigo DL-05, março, 2007.

[2] Craford, M. G. “LEDs challenge the incandescents,” IEEE Circuit Device Mag., vol.8, no.1, pp.24 -29 ,Aug. 1992.

[3] Chao-Lung Kuo; Tsorng-Juu Liang; Kai-Hui Chen; Jiann-Fuh Chen; , "Design and implementation of high frequency AC-LED driver with digital dimming," Circuits and Systems (ISCAS), Proceedings of 2010 IEEE International Symposium on , vol., no., pp.3713-3716, May 30 2010-June 2 2010.

[4] Loo, K. H., Lai, Y.M., Tse C. K., “Design and Analysis of LCC Resonant Network forQuasi-Lossless Current Balancing in Multistring AC-LED Array”, Transac. on Power Electronics, vol. 28, No. 2, February 2013.

[5] Hwu, K. I., Tu,W.C., Fang, Y.T., "Dimmable AC LED Driver With Ef ciency Improved
Based on Switched LED Module", Journal of Display Technology, vol. 10, no. 3, March 2014.
[6] Miskin, M. and Andersen J.N.; "AC Light Emitting Diode and AC LED Drive Methods and Appratus", United State Patent, 2009.
[7] Kang, E.; Kim, J.; Oh, D. and Min, D.; "A 6.8-W Purely-Resistive AC Light-Emitting Diode Driver Circuit with 95% Power Factor", 8th International Conference on Power Electronics (ECCE), 2011.
[8] Aoyama, Y., Yachi, T. "An LED Module Array System Designed for Streetlight Use," in Energy 2030 Conference, 2008. ENERGY 2008. IEEE, 2008, pp. 1-5.
[9] Kang, E., Kim, J., Oh D., Min, D., "6.8-W Purely-Resistive AC Light-Emitting Diode Driver Circuit with 95% Power Factor", 8th International Conference on Power Electronics – ECCE, Asia, 2011.
[10] Jiang, H., Lin, J., Jin, S., "Light Emitting Diodes for High AC Voltage Operation and General Lighting," U.S. Patent 6957899, Oct. 25, 2005.
[11] Jung, H.M., Kim J.H., Lee B.K., Yoo D.W. "A New PWM Dimmer Using Two Active Switches for AC LED Lamp", The 2010 International Power Electronics Conference, 2010.
[12] http://www.acriche.com/en/product/prd/acriche.asp
[13] Chun-An Cheng; Yuan-Min Cheng; , "A novel two-stage electronic ballast for metal-halide-type HID lamps," TENCON 2007 - 2007 IEEE Region 10 Conference , vol., no., pp.1-4, Oct. 30 2007-Nov. 2 2007.
[14] Fuerback A. L., Postiglione, C. S., Nascimento, C. B., Martins, D. C. Perin, A. J. "Near-Unity Power Factor Electronic Ballast Based on Integration Techniques to Drive High-Intensity Discharge Metal Halide (HID–MH) Lamps", IEEE Transactions on Industrial Electronics, vol. 59, no. 4, april 2012.
[15] Chun-An Cheng; Hung-Liang Cheng; Kuan-Lin Chu; Kun-Jheng Lin; Ping-Wen Wang; , "A compact, high-power-factor HID lamp ballast," Power Electronics and Drive Systems, 2009. PEDS 2009. International Conference on , vol., no., pp.967-972, 2-5 Nov. 2009.
[16] Holmes, D.G. and T.A. Lipo, Pulse Width Modulation for Power Converters – Principles and Practice. IEEE Press Series on Power Egineering, ed. M.E. El-Hawary. 2003: John Wiley & Sons.
[17] Malschitzky, A., Albuquerque, F., Agostini, E., Nascimento, C. B., "Single-Stage Integrated Bridgeless-Boost Non-Resonant Half-Bridge Converter for LED Driver Applications", IEEE Transactions on Industrial Electronics, vol. 65, no 5, pp. 3866 – 3878, May 2018.
[18] Sebastian, J., Cobos, J.A., Lopera, J.M., et al.: 'The determination of the boundaries between continuous and discontinous conduction modes in PWM DC-to-DC converters used as power factor pre-regulators', IEEE Trans. Power Electron., 1995, 10, (3), pp. 574–582.
[19] Simonetti, D.S.L., Sebastian, J., Uceda, J.: 'The discontinuous conduction mode sepic and cuk power factor preregulators: analysis and design', IEEE Trans. Ind. Electron., 1997, 44, (5), pp. 630–637.